Estimating Surface Soil Moisture in Simulated AVIRIS Spectra

Michael L. Whiting,[1, 2] Lin Li,[2] and Susan L. Ustin[2]

[1]USDA – Natural Resources Conservation Service, Davis, California 95616-4165
[2]Center for Spatial Technologies and Remote Sensing, University of California
Davis, California 95616-8671

1.0 INTRODUCTION

Soil albedo is influenced by many physical and chemical constituents, with moisture being the most influential on the spectra general shape and albedo (Stoner and Baumgardner, 1981). Without moisture, the intrinsic or matrix reflectance of dissimilar soils varies widely due to differences in surface roughness, particle and aggregate sizes, mineral types, including salts, and organic matter contents. The influence of moisture on soil reflectance can be isolated by comparing similar soils in a study of the effects that small differences in moisture content have on reflectance. However, without prior knowledge of the soil physical and chemical constituents within every pixel, it is nearly impossible to accurately attribute the reflectance variability in an image to moisture or to differences in the physical and chemical constituents in the soil. The effect of moisture on the spectra must be eliminated to use hyperspectral imagery for determining minerals and organic matter abundances of bare agricultural soils. Accurate soil mineral and organic matter abundance maps from air- and space-borne imagery can improve GIS models for precision farming prescription, and managing irrigation and salinity. Better models of soil moisture and reflectance will also improve the selection of soil endmembers for spectral mixture analysis.

Previous investigations have used laboratory spectra that are continuous throughout the full range to estimate moisture based on water absorption bands. Unfortunately, light is absorbed by water in the atmosphere, preventing the use of many of these bands in image spectra. In laboratory studies, it is common to relate soil moisture to specific water absorption overtones at 1.1, 1.4, 1.9 µm (Liu et al., 2002; Lobell and Asner, 2002). For image spectra it is necessary to utilize the general shapes of the spectra, properly calibrated for the atmosphere, excluding the individual absorptions of the water overtones.

Consistent with previous investigators, we noted the loss of reflectance with increasing water content (Bowers and Hanks, 1965); our spectra showed the same decline of albedo in Figure 1. The shape of the continuum in the VIR and SWIR responds, in a large part, to the water fundamental absorption in the 2.8 µm region (Bishop, 1988). The fundamental absorption of water affects the soil spectrum by spreading the absorption with increasing water bulk content (Bishop et al., 1994). We observed that as the overall reflectance declined, the position of the maximum reflectance also shifted to shorter wavelengths.

Currently available field and airborne instruments with a SWIR range to 2500 nm are just short of this fundamental water absorption peak. Therefore, it is necessary to model the SWIR continuum to extrapolate beyond the wavelength range of the instruments. Fitting a mathematical curve and linear functions to the extrapolated continuum provides numerical measures of the absorption depth and area changes in the fundamental water absorption. The shifting of the maximum reflectance to shorter wavelengths lengthens the tail of the curve as the absorption deepens. This shape response is characteristic of the changes seen in an inverted Gaussian function. Mineral and vegetation absorptions have been commonly measured through parameterizing the absorption bands with Gaussian functions (Miller et al., 1990; Mustard, 1992; Sunshine and Pieters, 1993).

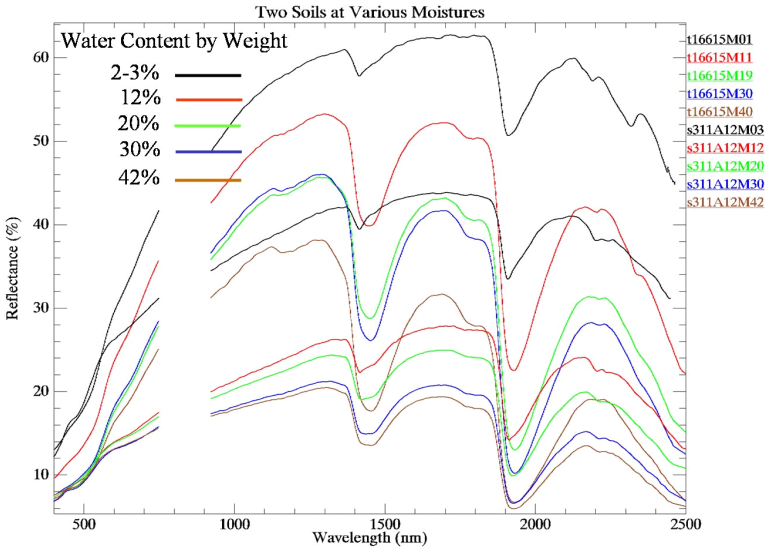

Figure 1. Distinctly different soils at similar moistures.

To demonstrate that water content can be estimated through its relationship

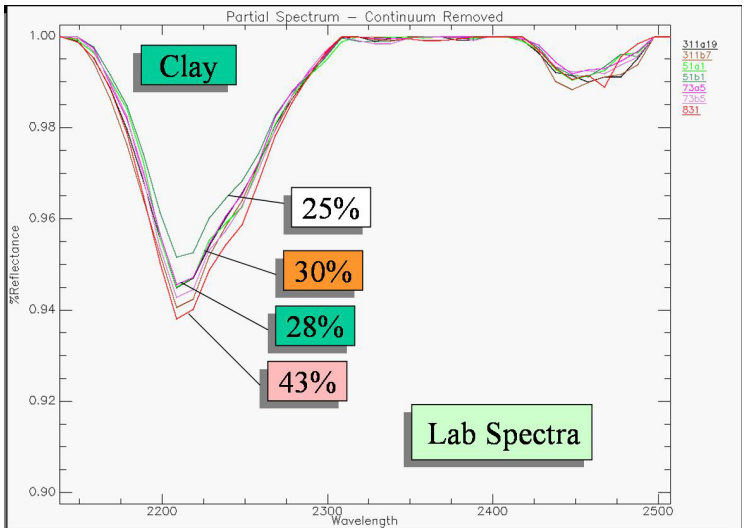

Figure 2. The absorption depth at 2200-nm is related to the clay contents.

to the fundamental absorption spread, laboratory soil spectra from a range Mediterranean soils and moisture contents were fitted to inverted Gaussian curves. The returned Gaussian parameters were regressed against the moisture contents of these soil samples. Several parameters from the Gaussian model were tested and demonstrated different levels of accuracy from 0.017 to 0.025 RMSE for estimating water content (g/g) (Whiting et al., in press).

Specific to the interest of this AVIRIS conference, determining whether AVIRIS has significant resolution for this modeling process is necessary before the process is applied to AVIRIS image. Eliminating the effect of soil water is essential to obtain accurate estimates of mineral and organic matter abundances. The first step in developing the correction for moisture effects is to accurately estimate moisture content. A large subset of these laboratory spectra were used to develop and validate the soil moisture Gaussian model (SMGM), degraded from 1-nm to 10-nm band widths, to simulate AVIRIS reflectance spectra. The regression of water content on these model parameters demonstrated even a slight improvement in estimating water content.

1.1 Effect of Moisture on Mineral Abundance Estimates

The depths of absorption near 2.2 µm increases corresponding to the increasing clay mineral contents when shown in the continuum removed spectra (Figure 2), obtained from similar soils in our study area. The shape of other absorption features has been associated with abundance, as in the derivatives of the 2.3 µm region in laboratory spectra data for carbonate abundance (Ben-Dor and Banin, 1990). The problem is that this contrast observed in the continuum is inconsistent with changes of water content, whether measured by the depth or shape.

As determined early on, the over-all reflectance of soil declines with increasing moisture (Figure 1). In contrast to increasing moisture absorption at 1.4 and 1.9 µm, mineral absorptions diminish, non-linearly, with increasing moistures as shown in continuum removed spectral from our study soils (Figure 3). Determining the correction for the spectra, and the mineral and organic matter absorptions, is part of our on-going research program.

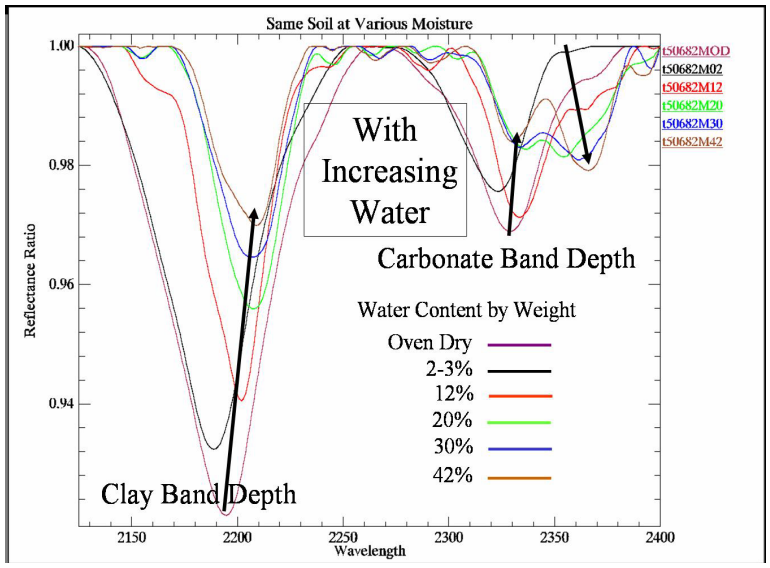

Figure 3. Absorption depth declines disproportionately to the amount of increasing water content, and decline in soil reflectance.

1.2 Physical and Mathematical Moisture Model

The decline in soil reflectance with increasing moisture follows a characteristic pattern, even among dissimilar soils. In Figure 1, the brighter soil from calcareous terraces in Spain and the darker soil from southern San Joaquin Valley, California basin rims, at the same moistures, appear to have very different continuum patterns. However, after the differences in intrinsic or matrix reflectance is eliminated by normalizing to the spectrum's maximum reflectance (Figure 4), the spectra from the same moistures show similar patterns, denoted by curved lines. Also,

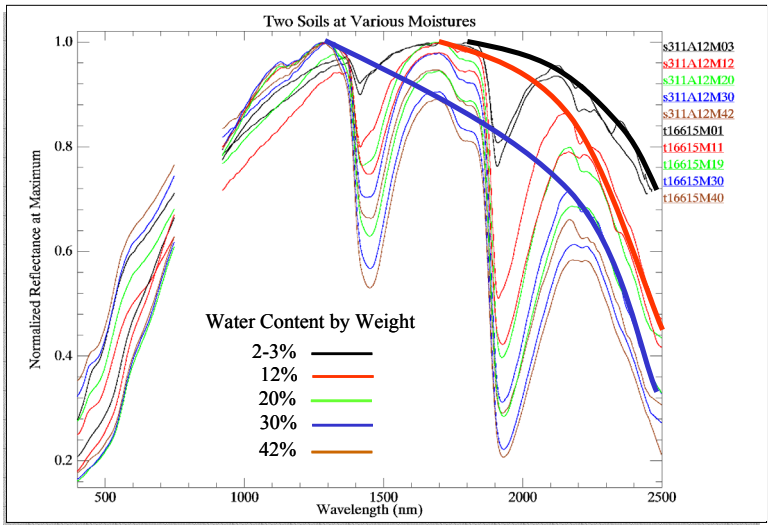

Figure 4. After spectra are normalized by maximum reflectance for each spectrum, the trend due to moisture becomes more apparent.

the maximum reflectance in the SWIR declines with increasing moisture content and the wavelength position of maximum shifts to shorter wavelengths, following the spread of the fundamental water absorption.

From the Beer-Lambert Law, we know that absorptions are log based, that is, absorbance is the negative log of reflectance. The difference from incident and reflectance light on soil (considered infinitely thick optically) is the portion absorbed. This apparent absorbance (Kortum, 1969) is equal to the product of a mineral's absorption coefficient and optical depth (Clark and Roush, 1984).

$$I = Io \exp(-ad) \text{ or } -ad = lnI - lnIo \quad (1)$$

where I is transmitted energy, Io, incident energy, *a,* absorption coefficient, and, *d* is the optical path length. While Hapke (1993) provides a number of techniques for converting reflectance to absorbance to reduce the effects of logarithmic compression, Yen et al. (1998) found the natural log the least unsatisfactory for linearizing reflectance data from laboratory measurements and transforming to apparent absorbance, defined by Kortum (1969) as the –ln(r). For the remainder of this discussion, the absorbed energy is described and modeled using the natural log of reflectance.

A common method of reduce complex shapes of absorptions to a few parameters is fitting the Gaussian Function (Miller et al., 1990; Sunshine and Pieters, 1993). The model has the advantages of parameterizing the absorption into three values: a) function center, b) its amplitude, and c) the distance to the inflection point. A fourth parameter can be derived, the area under the curve. After a series of trial and error, the position of the maximum reflectance was left unconstrained, which allowed the functional tail to shift with the spread of the fundamental water absorption. The spectra are normalized by dividing the reflectance at each band by this maximum reflectance (R_0). The center of function was constrained to 2.8μm (μ), the other parameters were determined through a least-squares fitting of the reflectance at each wavelength (λ_i), for the depth (R_d) or the amplitude of the Gaussian Function, and the distance to the inflection point (σ) in Equation (1).

$$g(\lambda) = R_0 - R_d * \exp\left\{\frac{-(\lambda_i - \mu)^2}{2\sigma^2}\right\} \quad (1) \qquad A = \int_{\lambda_0}^{\lambda_{max}} \frac{2\sigma^2 R_d}{-(\lambda_0 - \lambda)^2} \quad (2)$$

The area between the extrapolated Gaussian curve and its baseline was determined through integrating equation (1) from the maximum reflectance wavelength to the center of Gaussian curve, shown in Equation (2).

The continuum was found by defining the upper general shape of the spectrum through a convex hull algorithm. The hull boundary points, at wavelengths greater than the maximum reflectance, were used in an iterative least squares fitting algorithm to solve for the best Gaussian function for SWIR spectrum, returning both the Gaussian parameters and the minimum least squares fit errors (Figure 5). The root mean squared error (RMSE) of the fit was calculated using the least squares and the number of hull boundary points for each spectrum. IDL (Research Systems, Inc., Boulder, CO.) was used to program the functional fits and the error determinations. The Gaussian parameters and area were regressed against the gravimetric water contents to determine the moisture curve coefficients. The linear and non-linear regressions and statistical evaluations were conducted using S-Plus 2000 (Insightful Corporation, Seattle, Washington).

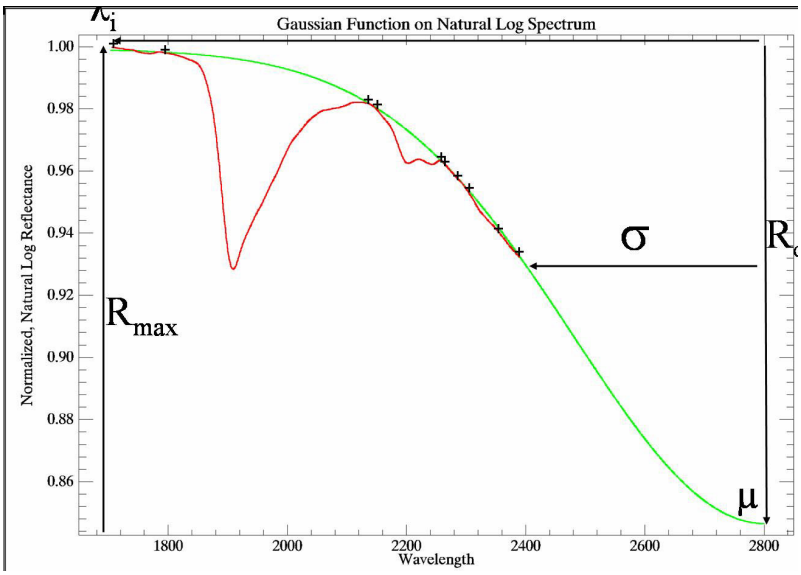

Figure 5. The Gaussian function fitting to a dry normalized soil spectrum.

2.0 STUDY METHOD

To evaluate the effectiveness of the Gaussian function to describe the response of the soil reflectance to moisture, the function was fitted to spectra from a variety of soils and a sequence moisture contents. The resulting Gaussian parameters were compared to a range of measured moistures, from oven dry to saturation.

2.1 Study Sites and Soil Sampling

Soils were from two distinctly different locations in Spain and California. The soils from Castilla-La Mancha, Spain, were collected from the calcareous uplifted Miocene calcareous and fill-cut terraces just south of the town of Tomelloso. These samples were stratified by their five landform surfaces, a) uplifted pedogenic carbonate terrace, b) internal drains on the upper terraces, c) and d) two lower level cut and fill alluvial terraces, and e) flood plain. In general, they are described as the upper fans or piedmont of "calizas y margas" (limestone and marls) mixed with "conglomerado arcilloso, coarzoso con gravas" (conglomerates of clays and gravels), (Martin et al., 1994). Sanchez et al. (1996) described the general types using the FAO soil classification system. Within the sampled area, the older surfaces of Petric Calcisols, limestone and marl with laminar calcareous crust, formed on alluvial fans, "developed from limestone and detritic materials of the upper Pliocene." In the younger alluvium and river wash, the soils are described as Haplic Calcisols, as calcisols lacking an argic B horizon and petrocalic horizon, "developed on detritic materials of alluvial bottom valleys." This map is general and designed for regional studies and planning.

The soils from the second region were formed on the basin rim of the Tulare Lake playa in the southern San Joaquin Valley, near the city of Lemoore, Kings County, California, United States. These samples were stratified by sodicity using (electro-conductivity, EC) and visible vegetation vigor or necrosis. The USDA Natural Resources Conservation Service described the soils as fine-loamy, mixed (calcareous), thermic Typic Torriorthents, and fine, montmorillonitic, thermic Typic Natrargrids using the USDA classification system (USDA, 1978). Their laboratory analysis described the mixed mineralogy of illite and montmorillonite clays.

Within the stratifications of both locations, one typical site was selected for modeling, where three samples were taken by transecting from west to east, at 10m apart. At a different location, more than a kilometer from the modeling site, an additional typical site was selected to collect one sample for validation.

These two regions provided soils with varying dry and moist colors, wide range of clay, and calcium carbonate and sodium chloride contents. Organic matter contents were similar, less than 2 % for both regions. Soils from the calcareous terraces in Tomelloso are bright due to adsorbed and free amorphous calcium carbonate. Pedogenic carbonate formations, from deep in the soil profile, have been exposed by erosion and surfaced by farm tillage practices. Carbonate aggregates, ranging in size from larger than gravels to finer than slit, are dispersed throughout the profiles. Younger cut-fill terraces and floodplains contained less carbonate and pedogenic gravels.

Soils in Lemoore differed in fine sand, silt and clay contents and in sodium chloride contents. The sodium contents promoted smooth surfaces through slaking of surface micropeds, and possibly influencing changes in the spectra (Courault et al., 1993). The Sodium Absorption Ratio (SAR) is the amount of sodium to the squared sum of calcium plus magnesium contents (Tanji, 1990) and ranged from 2.5 to 6.5 for Lemoore and 0.05 to 0.12 for Tomelloso. Though the mean for the basin high sodicity group is less than the minimum ratio of 15:1 for the sodic classification (SSSA, 1997), it is more than double the mean ratio of the low sodicity group, and one or two orders of magnitude greater than the Tomelloso region.

2.2 Collecting the Soil Spectra

In the laboratory, using a Cary 5E spectrophotometer (Varian Incorporated, San Jose, California) fitted with an external integrating sphere (Labsphere, Inc, North Sutton, New Hampshire) each moisture level of each samples was measured three times. The sample holders were mounted in the light-tight port at the base of the sphere. The instrument projected a collimated light onto the soil surface at nadir, with a constant reference double beam. The maximum relative reflectance was calculated from measurements of a white Spectralon panel (Labsphere, Inc, North Sutton, New Hampshire). The light from the spectrophotometer struck the targets in a fixed rectangle approximately 1 cm by 2.8 cm within the 3.5 cm diameter holder. To avoid any bias due to surface geometry, three measurements were made of the soil target. The holders were rotated approximately 60^{o} before the consecutive spectral measurements.

After lightly hand grinding with a mortar and pestle, two replicate samples were packed into small clear plastic petri dish sample holders. Spectra were collected at the air dry, then oven dry states. The collection of spectra continued after each of eleven additions of water, at approximately 5% water content intervals. At the end, the soils were returned to the desiccators to air dry, then oven dried and spectra were collected with each moisture change. Of the possible 3600 combinations of soil replicates and moisture contents, 45 samples, by 2 soil replicates, and 3 spectral measurements with each of 15 moistures, there were 3,462 acceptable measurements, with 2,619 used for modeling and 843 for validation. Some samples had fewer measurements because they saturated earlier than the others and did not need all 11 water additions. Additional spectral were discarded when the second oven dry weight for the soil replicate did not return to within 0.1% of the first oven dry weight. Either the initial weight was in error or sample material was lost with handling.

3.0 RESULTS AND DISCUSSION

3.1 Fitting the Moisture Model to Laboratory Spectra

The Gaussian parameters were determined for each spectra from the sequence of moistures and soil replicated samples, and then evaluated against the measured water contents. Of the spectra, the number of hull boundary points for each spectrum ranged from 20 to 100, with the greater numbers being from the drier replicates due to greater curvature in the spectra. The maximum reflectance moved from between 1650 and1800 nm for the dry soils to near 1300 nm for moist soils. There was not a gradation of maximum reflectance positions due to the deep water absorption at 1400 nm. The fitted Gaussian returned parameters of depth, distance to inflection and area under the shortward portion of the curve.

For all soils and all moistures, the area of the curve was the best predictor of moisture content. While the functional depth and distance to the inflection point predicted the water content less accurately, analyzed together as the integration of the area, the performance was far superior. The prediction accuracy for all parameters decreased with increased moisture, and significantly worsened above 0.30 water content. The increase in moisture begins to saturate the soil samples, filling the small pores then the larger pores (Jury et al., 1991). The reflectance from the water becomes dominate, instead of the soil and water (Liu et al., 2002).

Since the area was far superior in predicting the water content, further analysis was conducted with this parameter. From the increasing variability exhibited in the predictions by the functional parameters, the linear model developed from the area was restricted to air dry to near field capacity, 0.02 to 0.32 gm/gm water content. Field capacity is defined as the water content that free draining soil holds against gravity after 24 hours (Jury et al., 1991). Most soils reach field capacity between 0.25 and 0.40 gm/gm water content (Brady and Weil, 1996). Our value of 0.32 gm/gm was derived from the sudden increase in variability for values above 0.32. The “restricted” model also eliminated spectra where the error in the Gaussian fit exceeded 0.0125 RMSE. The same variability was apparent in the validation set. The restricted validation set had no spectra fit exceeding the 0.0125 RMSE, within the moisture contents below 0.32.

The restricted soil moisture Gaussian model (SMGM) for these spectra was highly correlated to water content, though the regression coefficients were slightly different for the two locations. The result of the model for all soils and moistures was coefficient of correlation (r^2) = 0.89, and for the restricted model set was $r^2 = 0.92$, and with stratifications within the study sites the r^2 improved in most to 0.95. The model for Lemoore has a slightly higher r^2 than that of Tomelloso.

The Lemoore soils are much more consistent between samples in texture and aggregate size. The Tomelloso varied widely between the geomorphic surfaces. The correlation coefficients for the Tomelloso restricted model and validation sets improved substantially by stratifying by the geomorphic surface. When the model was applied to the

validation set for only Lemoore the results were very similar to the modeling set, with r^2 of 0.92 and RMS of 2.85 in water content percentage. The fit lines for the restricted models for the two regions are shown in Figure 6.

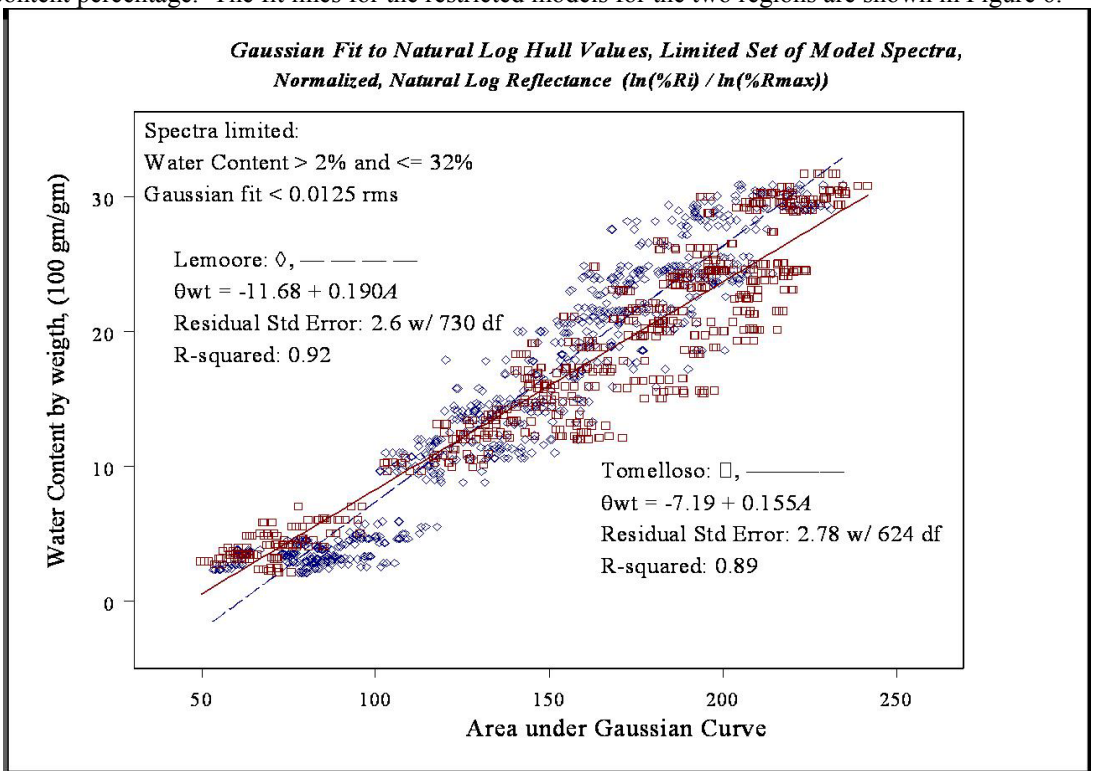

Figure 6. The linear fit of water content on the Gaussian area for Lemoore and Tomelloso soils.

3.2 Fitting the Model to Simulated AVIRIS Spectra

More relevant to this conference, we tested the effectiveness of this model at the 10-nm full width half maximum (FWHM) channels of AVIRIS data. The model and validation samples were selected to capture both saline-sodic and healthy vegetation responses determined from a pseudo-color infrared composite of a 1998 ER-2 AVIRIS image of the Sheely Farms, near Lemoore, California.

Resampling lab spectra has the advantage of studying the effects of spectral resolution without increasing the errors associated with incorrectly calibrated image data. The same lab spectrophotometer data between 400 nm and 2390 nm was interpolated to AVIRIS image band centers, which degraded the spectra from 1,990 1-nm bands to 189 nominal 10-nm bands. The resampling improved the smoothness of the spectra, though it reduced the range in the number hull boundary points from 20 to 100 in the full laboratory spectral to 5 to 20 in the simulated AVIRIS data. The fit to the Gaussian improved substantially with no error rate greater than 0.0125 RMS. With high moisture contents, the number of hull points for some spectra fell below 5, and the fitting with the Gaussian function would not converge. The number of hull points must be greater than the number of parameters in the function.

Table1. Comparison of laboratory and simulated AVIRIS spectra fitting and water content model prediction.

Comparison of RMS	Lab Spectral	AVIRIS-Sim
g(λ) to Hull Points	0.015	0.0125
R^2 – Limited Set	0.92	0.93
Area Fit to Water Content:		
Overall	3.7	4.4%
Limited Range	2.9%	2.9 %

The variability in the AVIRIS Gaussian parameters values was similar to the laboratory spectral data (Figure 7). While the amplitude of the function, again, was correlated to the water content, the area of Gaussian was a better predictor of the water content. In Table 1, the laboratory restricted model and the AVIRIS simulation model are basically the same, though there is a slight difference in the off-set coefficient, -1.68 to -11.81, and the same 0.19 coefficient for the area. The r^2 is virtually the same for both, 0.92 to 0.93, respectively.

When the model is applied to the validation spectral set, the accuracy of the model was similar to the model set for all moisture contents and is within RMS of 4.4 %-water

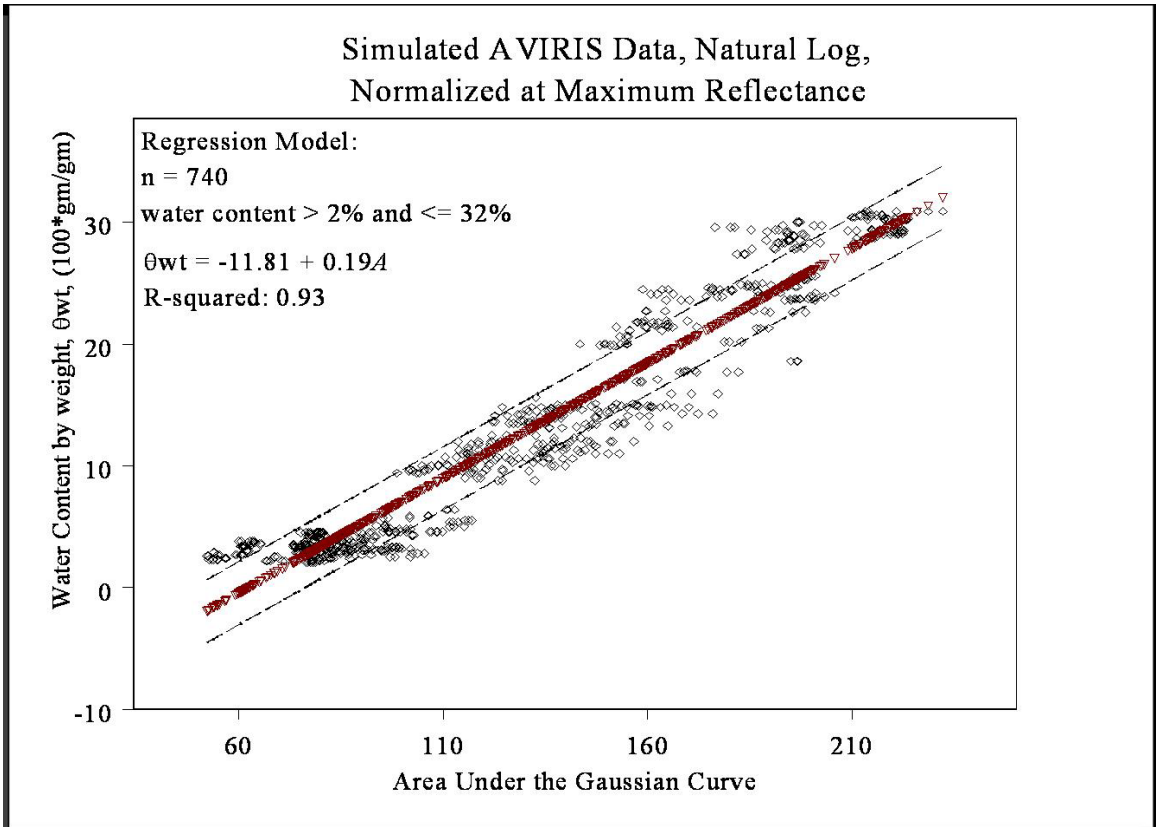

Figure 7. Similar linear fit of water content for the AVIRIS spectra simulation.

content. Again, the model is much improved within a restriction of the range of the water contents from 0.02 to 0.32 with the RMS falling to 2.84 %-water content.

4.0 CONCLUSIONS

The general shape of soil spectra SWIR region is related to water's fundamental absorption slightly beyond the spectral range of our field and imagery instruments. The fundamental absorption can be modeled with a Gaussian function on the hull boundary points of the continuum by extrapolating the SWIR continuum to the region of fundamental water absorption. The function and change of the SWIR general shape are sufficiently sensitive to the water content changes. Within the sandy loam to clay loam textures, in widely diverse Mediterranean soils from California and La Mancha, Spain, and common moisture ranges, the area under the curve has a linear relationship that can accurately estimate the surface moisture content within 3 %-water content (RMSE).

Specific to the application of this model for the retrieval of soil water content to imaging spectrometer data, the 10-nm FWHM of AVIRIS data appears to have sufficient detail to return the same accuracies. Smoothing, induced by the interpolation of resampling, did improve the fit accuracy slightly. At the higher moisture contents, some spectra had a reduced the number of hull boundary points, less than the needed number of the parameters, and fail to converge. Investigations are continuing on using the model of eliminate the effects of soil moisture to improve the estimates of other soil constituents in the soil spectra.

5.0 ACKNOWLEDGEMENTS

Contributions by JPL-NASA of ER-2 and Twin Otter flights with AVIRIS over the Sheely Farm in Lemoore are gratefully acknowledged. Also, the researchers wish to thank the USDA, Natural Resources Conservation Service for the staff time provided through an Interagency Personal Agreement with University of California, Davis. A portion of this study was funded by NASA EOS grant #NAG5-9360. The cooperation of Ted Sheely, of AzCal Farm Management, is greatly appreciated.

6.0 REFERENCES

Ben-Dor, E., and Banin, A. 1990. "Near-infrared reflectance analysis of carbonate concentration in soils," Applied Spectroscopy, vol. 44, no. 6, pp. 1064-1069.

Bishop, J. L. 1988. "The effects of water, octahedral cation substitution and exchangeable cation composition on the shortwave infrared reflectance spectrum of montmorillonite," M.S. Thesis, Stanford University, Stanford, California.

Bishop, J. L., Pieters, C. M., and Edwards, J. O. 1994. "Infrared spectroscopic analyses on the nature of water in montmorillonite," Clays and Clay Minerals, vol. 42, no. 6, pp. 702-716.

Bowers, S. A., and Hanks, R. J. 1965. "Reflection of radiant energy from soils," Soil Science, vol. 100, no. 2, pp. 130-138.

Brady, N. C., and Weil, R. R. 1996. *The Nature and Properties of Soils*, Prentice Hall, Upper Saddle River, NJ.

Clark, R. N., and Roush, T. L. 1984. "Reflectance spectroscopy: Quantitative analysis techniques for remote sensing applications," Journal of Geophysical Research, vol. 89, no. B7, pp. 6329-6340.

Courault, D., Bertuzzi, P., and Girard, M. C. 1993. "Monitoring surface changes of bare soils due to slaking using spectral measurements," Soil Science Society of America Journal, vol. 57, pp. 1595-1601.

Hapke, B. 1993. *Theory of Reflectance and Emittance Spectroscopy*, Cambridge Univ. Press, New York.

Jury, W. A., Gardner, W. R., and Gardner, W. H. 1991. *Soil Physics*, John Wiley & Sons, Inc., New York.

Kortum, G. 1969. *Reflectance Spectroscopy*, Springer-Verlag, New York.

Liu, W., Baret, F., Gu, X., Tong, Q., Zheng, L., and Zhang, B. 2002. "Relating soil surface moisture to reflectance," Remote Sensing of Environment, vol. 81, pp. 238-246.

Lobell, D. B., and Asner, G. P. 2002. "Moisture effects on soil reflectance," Soil Science Society of America Journal, vol. 66, pp. 722-727.

Martin, J. L. B., Saenz, M. C., Crues de Abia, J., Portillo, A., and Madurga, M. R. L. 1994. "Hidogeologia," *Desertificacion en Castilla-La Mancha, El Proyecto EFEDA*, F. M. Manas, ed., Universidad de Castilla-La Mancha, Albacete, Spain, pp. 71-96.

Miller, J. R., Hare, E. W., and Wu, J. 1990. "Quantitative characterization of the vegetation red edge reflectance 1. An inverted-Gaussian reflectance model," International Journal of Remote Sensing, vol. 11, no. 10, pp. 1755-1773.

Mustard, J. F. 1992. "Chemical analysis of actinolite from reflectance spectra," American Mineralogist, vol. 77, pp. 345-358.

Sanchez, J., Boluda, R., Morell, C., Colomer, J. C., Artigao, A., and Tebar, J. I. 1996. "2.1. Assessment of soil degradation in desertification threatened areas: a case study in Castilla-La Mancha (Spain)," *EFEDA-II. Final Report: Desertification processes in the Mediterranean Area and their interlinks with the global climate*, F. M. Manas, ed., Universidad de Castilla-La Mancha, Albacete, Spain, pp.19-53.

SSSA. 1997. *Glossary of Soil Science Terms*, Soil Science Society of America, Madison, WI.

Stoner, E. R., and Baumgardner, M. F. 1981. "Characteristic variations in reflectance of surface soils," Soil Science Society of America Journal, vol. 45, pp. 1161-1165.

Sunshine, J. M., and Pieters, C. M. 1993. "Estimating modal abundances from the spectra of natural and laboratory pyroxene mixtures using the modified Gaussian model," Journal of Geophysical Research-Planets, vol. 98, no. 5, pp. 9075-9087.

Tanji, K. K. 1990. *Agricultural Salinity Assessment and Management*, ASCE Manuals and Reports on Engineering Practice No. 71, American Society of Civil Engineers, New York, pp. 619.

USDA, NRCS. 1978. *Soil Survey Kings County, California*, USDA Soil Conservation Service in cooperation with University of California Agricultural Experimental Station, Hanford, CA.

Whiting, M. L., Li, L., and Ustin, S. L. in press. "Predicting Water Content Using Gaussian Model on Soil Spectra," Remote Sensing of Environment.

Yen, A., Murray, B., and Rossman, G. 1998. "Water content of the Martian soil: Laboratory simulations of reflectance spectra," Journal of Geophysical Research-Planets, vol. 103, no. E5, pp. 11125-11133.